

# Colloidal processing of BaTiO<sub>3</sub> using ammonium polyacrylate as dispersant

Carlos Gómez-Yáñez, Heberto Balmori-Ramírez\*, Froylán Martínez

*Department of Metallurgical Engineering, ESQIE, Instituto Politécnico Nacional, A.P.75-593, México City 07738, Mexico*

Received 12 July 1999; received in revised form 9 August 1999; accepted 19 September 1999

## Abstract

The variation of the  $\zeta$  potential of BaTiO<sub>3</sub> particles in aqueous suspension as a consequence of changing the pH and the concentration of ammonium polyacrylate (NH<sub>4</sub>PA) has been studied. An isoelectric point at pH  $\sim$ 2.5 was found. The  $\zeta$  potential decreases upon addition of NH<sub>4</sub>PA up to 0.1 g of dispersant/g of powder. Using sedimentation tests, it was found that the stabilization of suspensions is attained at pH greater than or equal to 8 and concentrations greater than or equal to  $1.5 \times 10^{-3}$  g of dispersant/g of powder. By rheological measurements, a pseudoplastic behavior and little thixotropy was observed in the suspensions. The maximum solid content attained during this work was 48 vol%. Infrared spectroscopy of the sedimented and dried powder was carried out. It was observed the presence of BaCO<sub>3</sub> and the change of ionization of the NH<sub>4</sub>PA molecules when the pH changes. High green density values (up to  $\sim$ 60% of the theoretical density) in BaTiO<sub>3</sub> cakes were achieved at pH of 11.3, at  $2.5 \times 10^{-3}$  g of dispersant/g of powder and with a solid content between 40 and 48 vol%. © 2000 Elsevier Science Ltd and Techna S.r.l. All rights reserved.

**Keywords:** A. Slip casting; A. Suspensions; D. BaTiO<sub>3</sub> and titanates

## 1. Introduction

BaTiO<sub>3</sub> is a widely used material in the electronic industry. With this material, high-capacitance capacitors, thermistors, and piezoelectric and humidity sensors are fabricated [1]. The electrical properties of the final BaTiO<sub>3</sub> devices depend on the microstructural characteristics. It has been observed that the dielectric constant increases when either the average grain size decreases or the density increases [2]. On the other hand, some porosity is necessary to maximize the PTCR effect [3]. Then, a careful microstructural control is essential when specific electric requirements have to be fulfilled. In turn, the microstructure is a function of the manufacturing process. Some common consolidation techniques such as uniaxial pressing could render a non homogeneous microstructure due to frictional effects between the powder and the die. Among the commercial consolidation techniques, colloidal processing along with

slip casting can provide a homogeneous microstructure in the devices, which allows better quality control [4]. Colloidal processing consists in the preparation of suspensions by mixing the ceramic powder, a solvent and an organic agent used as dispersant. The technique is focused to achieve the complete dispersion of the ceramic particles in the liquid medium. However, the interaction among the solvent, the powder and the dispersant is rather complex, so a comprehensive study should be carried out in order to understand the interaction among these components and to find the conditions where the ceramic particles are well dispersed. Once stable suspensions are prepared under the proper conditions, the suspensions are cast into porous molds and high green density pieces can be obtained [4]. In case of BaTiO<sub>3</sub>, colloidal processing in aqueous media has been studied [5–9]. Since colloidal processing is widely used in tape casting, studies of BaTiO<sub>3</sub> suspensions in organic media have also been done [10–14]. The present work focuses on the colloidal processing of BaTiO<sub>3</sub> in aqueous media using ammonium polyacrylate as dispersant to determine the conditions where the powder is dispersed. The influence of solid content on the green density of slip-cast bodies is also studied. Ammonium

\* Corresponding author. Tel.: +525-729-6000, ext. 54207; fax: +525-729-6000, ext. 55270.

E-mail address: hbalmoni@andromeda.esiqie.ipn.mx (H. Balmori-Ramírez).

polyacrylate ( $\text{NH}_4\text{PA}$ ) is a commercial dispersant that has been successfully used to disperse alumina and zirconia powders in water [15–17].

## 2. Experimental procedure

### 2.1. Characterization of the powder

#### 2.1.1. Powder

The shape and size of the  $\text{BaTiO}_3$  (Merck 12048) particles were analyzed by scanning electron microscopy (JEOL 6300) and the chemical composition by wet chemical methods and energy dispersive spectroscopy (EDS) (Noran 92).

### 2.2. Stabilization conditions

#### 2.2.1. $\zeta$ Potential

The aim of this study was to find the conditions for a possible electrostatic stabilization in the suspensions, and to observe the dispersant influence on the particle surface electric charge. In a polypropylene matrass, 1 l of 1 wt% mixture of deionized water and  $\text{BaTiO}_3$ , adding  $10^{-3}$  molar of KCl as electrolyte was prepared. The pH was fixed using either  $\text{NH}_4\text{OH}$  or  $\text{HNO}_3$ . The concentrations of these reactives were chosen in such a way that the minimum volume of reactive was used, then, the reactives were sometimes diluted and sometimes concentrated. The mixture was stirred with a magnetic stirrer for 24 h, during this time, the pH was adjusted until the desired value (1.5, 2.7, 6.3, 10.3 and 11.3) did not change. After conditioning, the mixture was divided in 5 aliquots in polypropylene matrasses. A determined amount ( $10^{-4}$ ,  $10^{-3}$ ,  $2 \times 10^{-3}$  and  $10^{-2}$  g of dispersant/g of powder) of  $\text{NH}_4\text{PA}$  (A-6114 Chukyo Yushi Co., Nagoya, Japan, 39.41 vol% in water) was added in each aliquot and the mixtures were stirred with a magnetic stirrer for 5 h, then the  $\zeta$  potential was measured in a Zetasizer 4 (Malvern Instruments). 30 measurements were made for each sample.

#### 2.2.2. Sedimentation

In the  $\zeta$  potential studies it is not possible to observe the steric stabilization due to the  $\text{NH}_4\text{PA}$  hence, sedimentation tests were performed. In this case, aqueous suspensions of 3 vol% of powder were prepared. The suspensions (100 ml) were milled during 1 h in a polyethylene ball mill (250 ml) with zirconia balls. During this hour of milling, the pH was fixed by adding either  $\text{NH}_4\text{OH}$  or  $\text{HNO}_3$ . Then the  $\text{NH}_4\text{PA}$  was added, and the milling continued for 23 h more. After conditioning for 24 h, the suspensions were poured in 100 ml glass test tubes that were sealed in the upper part to minimize the liquid lost by water evaporation. When the sedimentation of the powder in suspension started,

an interface between a clear water layer and a cloudy region appeared. The height of such interface was measured as a function of the elapsed time.

### 2.2.3. Rheology

In the slip cast technique, high solid contents ( $\sim 50$ – $60$  vol%) are used but sedimentation tests cannot be realized at these concentrations. For this reason, several suspensions were prepared at conditions where they could be cast and the rheological characteristics were studied. Rheological tests permit to identify the conditions where the suspensions are better dispersed. For these tests, suspensions were prepared with solid contents from 40 to 48 vol%; these suspensions were ball-milled as indicated above. After conditioning, the suspensions were degassed in a bell jar using a mechanical vacuum pump, during 30 min. Then the suspensions were poured in a rheometer of concentric cylinders (Haake, RV-20, RC-20) which is able to control the shear rate and measure the corresponding shear stress. The shear rate was applied from 0 to  $100 \text{ s}^{-1}$  in 3 min, then  $100 \text{ s}^{-1}$  during 3 min and finally from 100 to  $0 \text{ s}^{-1}$ . This program had the following intention: in the shear rate plateau, the structures that formed during the increment of the shear rate have the opportunity to change to different configurations, i.e. it is possible to observe a dependence of viscosity with time (thixotropy). The rheological studies were carried out at pH of 8.5, 10 and 11, at 30, 40 and 45 vol% of solids, and  $10^{-3}$ ,  $2.5 \times 10^{-3}$ , and  $2 \times 10^{-2}$  g of dispersant/g of powder.

### 2.2.4. Infrared spectroscopy

An infrared spectroscopy study was carried out to observe the interactions among the components of the suspensions. Samples for infrared spectroscopy studies were taken from the sediment formed during the sedimentation tests. The supernatant water was extracted with a pipette and the test tubes were introduced in a stove at  $75^\circ\text{C}$ . The powders were milled in an agate mortar once they were dry, and were then introduced in an Infrared Spectrometer (Perkin–Elmer, System 2000, FT-IR).

### 2.3. Slip casting

#### 2.3.1. Slip casting

When the dispersion conditions were known from the above described studies, slip casting of the suspensions followed. The suspensions to be cast were prepared in the same manner as those used in the rheology studies. The suspensions were cast in small bores ( $1.5^\circ$  conic) made in a Lucite plate (25 mm thick) which was fixed on a Plaster of Paris plate. Once the water of the suspensions was filtered, the cakes were calcined at  $1000^\circ\text{C}$  during 1 h using a heating rate of  $10^\circ\text{C}/\text{min}$ . To characterize the green structure of the cast pieces, mercury porosimetry (Micromeritics 9410) was used.

### 3. Results

#### 3.1. Powder characterization

##### 3.1.1. Powder

In Fig. 1 a micrograph of the  $\text{BaTiO}_3$  particles is presented. Their shape is rounded and the average particle size is  $0.45 \mu\text{m}$ . A compositional Ba/Ti ratio of 0.88 was found by EDS.

#### 3.2. Stabilization conditions

##### 3.2.1. $\zeta$ potential

In Fig. 2 the  $\zeta$  potential of the  $\text{BaTiO}_3$  particles as a function of the pH is presented. An isoelectric point was found at  $\text{pH} \sim 2.5$ . The surface of the  $\text{BaTiO}_3$  particles are positively charged at lower pH values and negatively at higher pH values. The highest  $\zeta$  potential value is presented in the basic pH region. Therefore, stabilization is probable at these pH values.

The change of the  $\zeta$  potential when the dispersant is added at constant pH is shown in Fig. 3. The  $\zeta$  potential decreases with an increment of dispersant and the effect is minimum at basic pH.

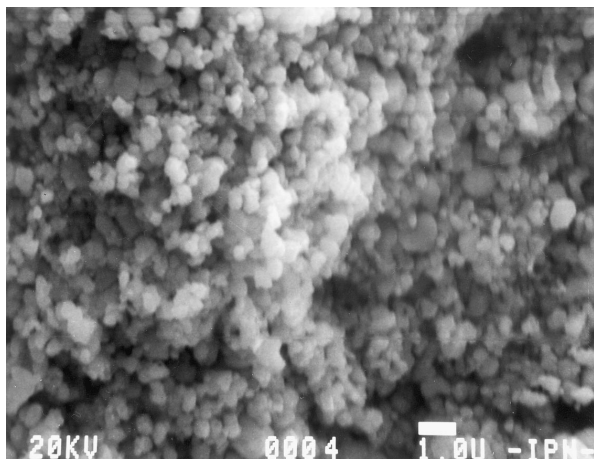


Fig. 1. Micrograph of the  $\text{BaTiO}_3$  powder.

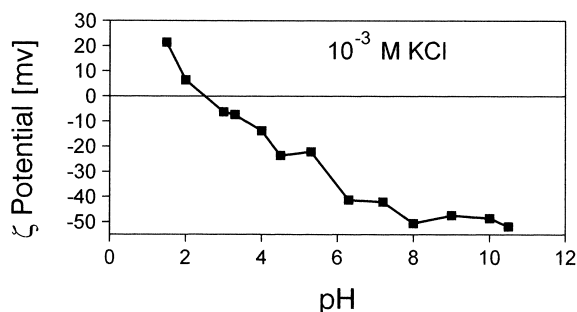


Fig. 2.  $\zeta$  Potential against pH in aqueous suspensions of  $\text{BaTiO}_3$  without dispersant.

##### 3.2.2. Sedimentation

Sedimentation curves for pH of 1.5, 8 and 10 are shown in Fig. 4(a)–(c). Some time after pouring the suspensions into the test tube, an interface was evident between a perfectly clear water region, at the top of the tube, and a cloudy region. The suspensions were considered stabilized when such interface was at 2 cm or more from the bottom of the test tube after  $10^4$  min ( $\sim 7$  days). As observed in Fig. 4(a), the dispersant did not contribute

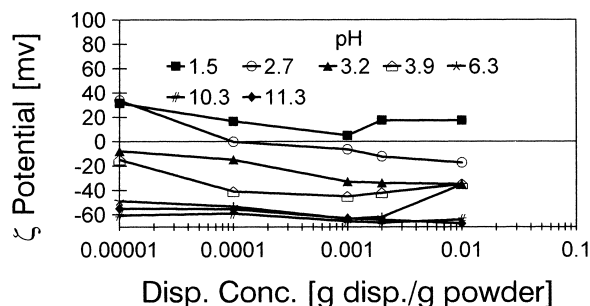


Fig. 3.  $\zeta$  Potential against ammonium polyacrylate concentration at different pH values.

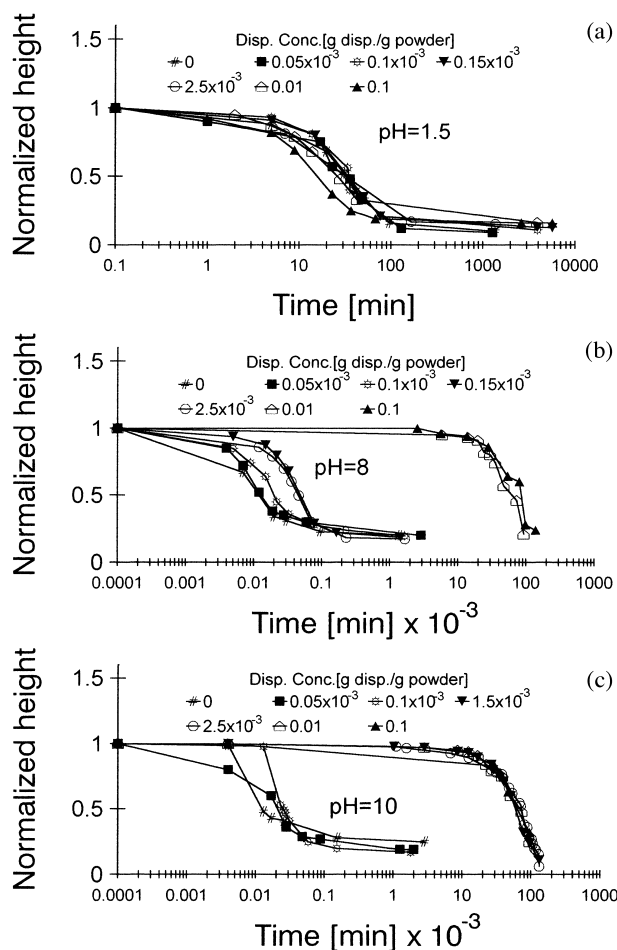


Fig. 4. Sedimentation curves for aqueous suspensions of  $\text{BaTiO}_3$  using ammonium polyacrylate as dispersant at pH of (a) 1.5, (b) 8 and (c) 10.

to the stabilization of the suspension at pH=1.5 and this lack of influence was also observed at pH of 3 and 6. However, stabilization was achieved at pH of 8 and at concentrations of dispersant higher than or equal to  $10^{-2}$  g of dispersant/g of powder [Fig. 4(b)]. At higher pH [Fig. 4(c)] a smaller amount of dispersant was needed to stabilize the suspension. It is word to notice that even at high pH it was necessary to add dispersant to stabilize the suspension in spite of the high  $\zeta$  potential values displayed by the powder, i.e. electrostatic stabilization was not possible in these suspensions.

Once the height of the cloudy layer did not change, this height was taken as the final sediment height. The final sediment height for each sample is presented in Fig. 5. Since the amount of powder was the same in all tubes, a small final sediment height means a more compact packing, which in turn indicates a high degree of dispersion in the suspension. As observed in Fig. 5, the smallest final sediment heights were obtained at high pH and high concentrations of dispersant.

Using the sedimentation curves and the  $\zeta$  potential results, a stability map was constructed in terms of pH and dispersant concentration (Fig. 6). When a relatively high concentration of dispersant (0.01 and 0.1 g dispersant/g powder) was used in some suspensions, it was

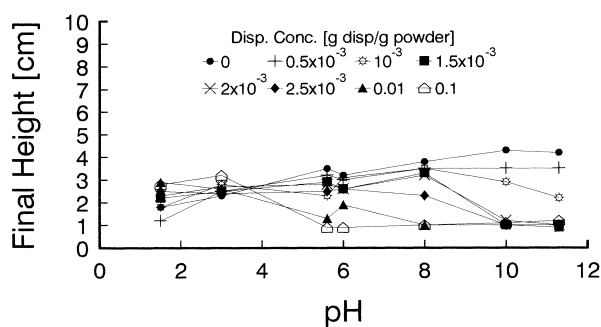


Fig. 5. Final sediment heights in sedimentation tests of BaTiO<sub>3</sub> aqueous suspensions using ammonium polyacrylate as dispersant. A solid content of 3 vol% was used.

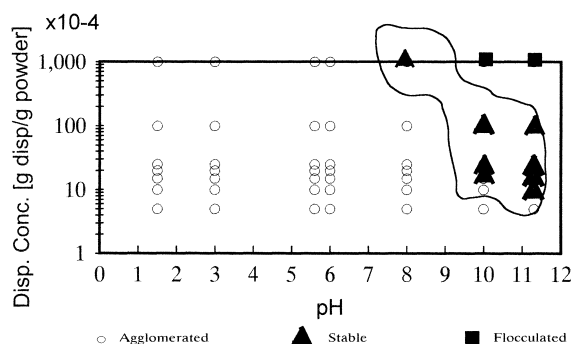


Fig. 6. Stability map of aqueous suspensions of BaTiO<sub>3</sub> in terms of pH and concentration of ammonium polyacrylate.

observed that an additional layer formed very fast (less than 5 min after pouring), below the cloudy layer mentioned above. In Fig. 6, these conditions were marked with a square symbol. The map presented in Fig. 6 shows a relatively narrow region of dispersion in the suspension. In this region then, the rheology studies were made and slip cast was attempted.

### 3.2.3. Rheology

An example of the typical shear stress vs. shear rate curves displayed by the suspensions prepared in this work is shown in Fig. 7. The curve is presented for the increment and decrement of the shear rate. The behavior observed denotes shear thinning, i.e. the viscosity decreases as the shear rate increases. In Fig. 8(a)–(c), it is observed how the viscosity changes when the pH, the concentration of dispersant and the solid content vary. To make comparisons, the value of viscosity at a shear rate of  $10 \text{ s}^{-1}$  was taken, which is approximately the shear rate applied in manual slip casting.

### 3.2.4. Infrared spectroscopy

The infrared spectra of the sedimented and dried powders appear in Fig. 9(a)–(c). The purpose of this study was to analyze the interaction among the components of the suspension, for this reason the analysis was limited in the range  $1520\text{--}1800 \text{ cm}^{-1}$  of wave numbers. In this region of the spectrum, five peaks appear. The peak appearing at  $\sim 1751 \text{ cm}^{-1}$  [Fig. 9(a)–(c)] coincides with one of the peaks of the BaCO<sub>3</sub> spectrum [8,18]. The origin of this BaCO<sub>3</sub> is controversial. It has been said that some ionic Ba<sup>2+</sup> is produced by the marginal dissolution of BaTiO<sub>3</sub>, and since the reaction between the ionic Ba<sup>2+</sup> in aqueous suspension and the CO<sub>2</sub> of the atmosphere at high pH value has been demonstrated, BaCO<sub>3</sub> is formed [19]. Other interpretation establishes that the BaCO<sub>3</sub> is normally present as contaminant in BaTiO<sub>3</sub> [6,7]. What is clear is that the presence of unreacted ionic Ba<sup>2+</sup> increases at low pH [7,20]; at high pH the concentration of ionic Ba<sup>2+</sup> should be low

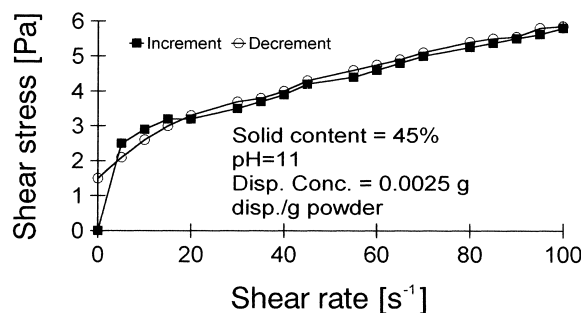


Fig. 7. Typical shear rate against shear stress curve of the aqueous suspensions of BaTiO<sub>3</sub> found during this work. This particular curve was obtained with 45 vol% of solid content, pH = 11, and  $2.5 \times 10^{-3}$  g dispersant/g powder.

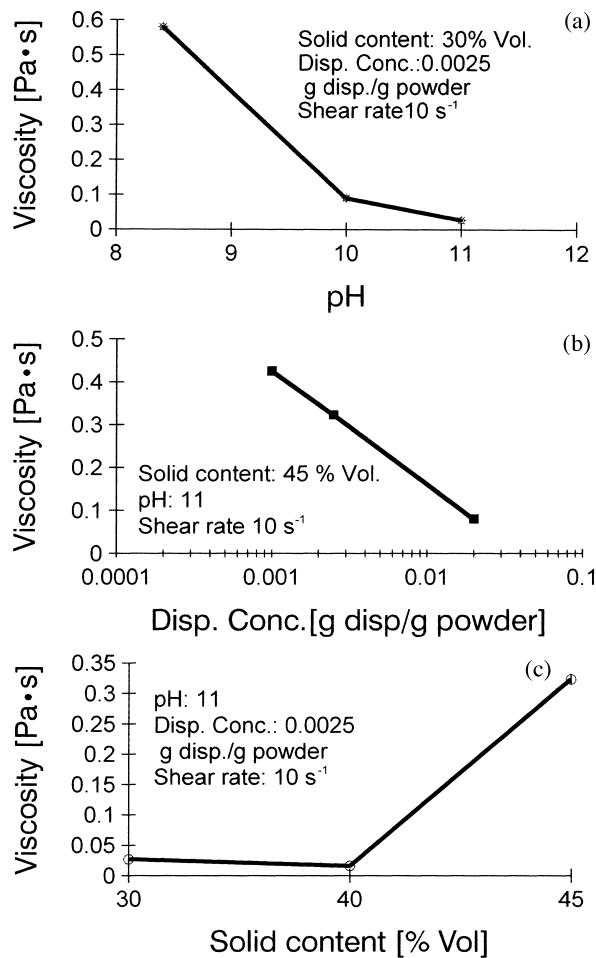


Fig. 8. Viscosity of the BaTiO<sub>3</sub> suspensions as a function of (a) pH, (b) dispersant concentration and (c) solid content.

therefore the present results suggest that the BaCO<sub>3</sub> is a contaminant. When the HNO<sub>3</sub> is added to the suspensions with the purpose of changing the pH, Ba(NO<sub>3</sub>)<sub>2</sub> is formed, then the peak at ~1751 cm<sup>-1</sup> disappears and the peak at ~1774 cm<sup>-1</sup> appears, which corresponds with the spectrum produced by the radical NO<sub>3</sub><sup>-1</sup> [18]. The band centered at 1636 cm<sup>-1</sup> is related to the vibration of H–O of the water [21] in which the NH<sub>4</sub>PA is dissolved. Two more peaks appear at ~1716 and ~1558 cm<sup>-1</sup> that are not present in the spectrum without dispersant; therefore these peaks must be produced by the dispersant. The peak at ~1716 cm<sup>-1</sup> is present at low pH while the peak at ~1558 cm<sup>-1</sup> is more noticeable at high pH.

### 3.3. Slip casting

Information relevant to the cast pieces is presented in Table 1. All these casting conditions are located within the stable region identified in the stability map (Fig. 6) Suspensions prepared at pH lower than 9.5 and with solid content higher than 48% were too thick to be cast. According to Table 1, when 10<sup>-2</sup> g of dispersant/g of

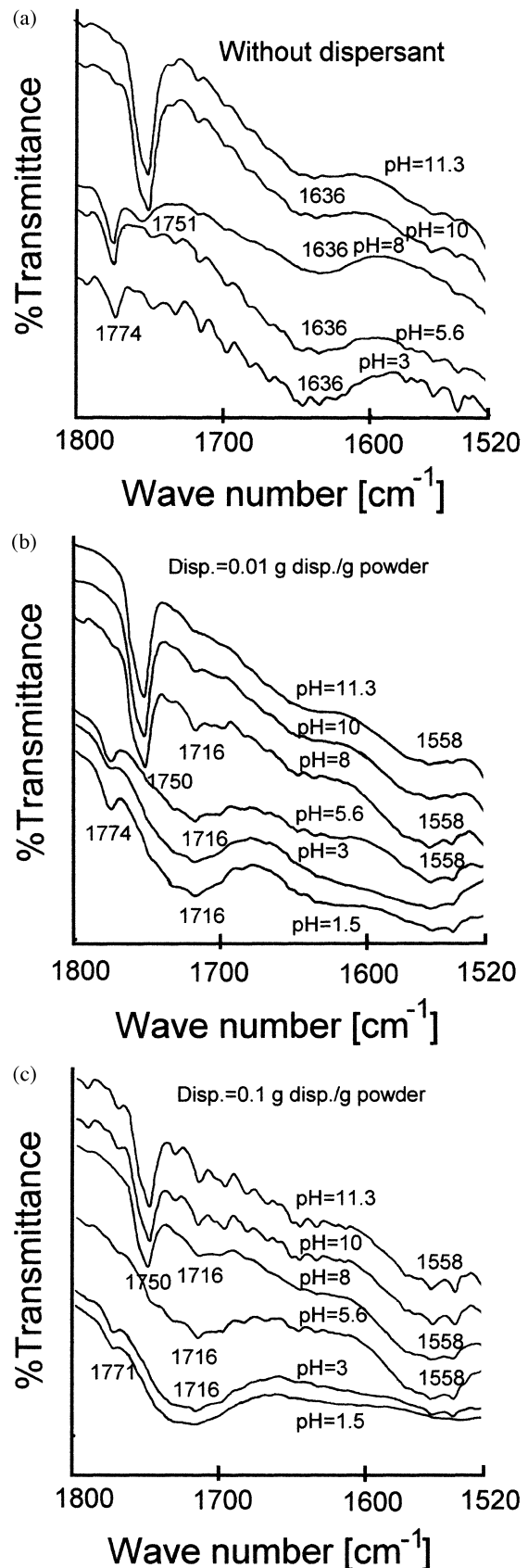


Fig. 9. Infrared spectra of the BaTiO<sub>3</sub> powder from suspensions prepared at different ammonium polyacrylate concentrations: (a) without dispersant, (b) 10<sup>-2</sup>, and (c) 10<sup>-1</sup> g of dispersant/g of powder.

Table 1  
Characteristics of green pieces cast at different conditions

PH	Conc. of dispersant (g disp./g powder)	Solid content (vol%)	Relative density <sup>a</sup> (% $\rho_{th}$ )	Open porosity (vol%)	Closed porosity (vol%)	Mean pore size ( $\mu\text{m}$ )	Minimum pore size ( $\mu\text{m}$ )	Maximum pore size ( $\mu\text{m}$ )
9.5	$10^{-2}$	45	51.91	47.14	0.95	0.32	0.07	0.50
10.5			53.74	45.69	0.55	0.25	0.07	0.30
11.3			51.86	47.14	0.58	0.31	0.06	0.40
11.3	$10^{-3}$	45	57.41	41.90	0.70	0.20	0.05	0.25
	$2.5 \times 10^{-3}$		59.79	37.81	2.40	0.14	0.06	0.20
	$10^{-2}$		51.86	47.14	0.58	0.31	0.06	0.40
11.3	$2.5 \times 10^{-3}$	40	57.79	42.31	0.00	0.25	0.07	0.30
		45	59.79	37.81	2.40	0.14	0.06	0.20
		48	57.99	40.47	1.54	0.21	0.07	0.30

<sup>a</sup> Theoretical density ( $\rho_{th}$ ) of  $\text{BaTiO}_3 = 6.01 \text{ g/cm}^3$ .

powder is used, lower green densities are attained, than at smaller amounts of dispersant. With lower concentration of dispersant, higher green densities are obtained, but the tendency of the density as a function of either the solid content or the concentration of dispersant is not clear. The mean pore diameter values are between 0.14 and 0.32  $\mu\text{m}$ . Three samples cast at the same conditions showed that there is at least a variability of  $\pm 0.05 \mu\text{m}$  in the mean values.

## 4. Discussion

### 4.1. Stabilization conditions

#### 4.1.1. $\zeta$ Potential

Since  $\text{BaCO}_3$  has been found in this kind of suspensions, the interpretation of Fig. 2 is rather difficult. In the studies of aqueous suspensions of  $\text{BaTiO}_3$  several isoelectric points have been reported; at  $\text{pH} \sim 7$  [6], at  $\text{pH} \sim 3$  [22] and  $\text{pH} \sim 4$  [9], and some researchers have not found any isoelectric point [5]. In this work, as can be seen in Fig. 2, the isoelectric point is at  $\text{pH} \sim 2.5$ , which is close to that reported in Ref. [22]. On the other hand, the compositional ratio  $\text{Ba/Ti} = 0.88$  implies that there is an excess of Ti. In case that this excess is present as  $\text{TiO}_2$ , which is not soluble in water, the expected effect on the isoelectric point could be a shifting to higher pH [23]. When  $\text{HNO}_3$  is added to the suspension, the pH decreases and  $\text{H}_3\text{O}^{+1}$  ions are formed. These ions could nullify some negative charges on the surface of the  $\text{BaTiO}_3$  particles so the  $\zeta$  potential shows a more positive value. On the contrary, when  $\text{NH}_4\text{OH}$  is added the pH increases and the  $\text{OH}^{-1}$  ions formed could neutralize positive charges on the surface of the  $\text{BaTiO}_3$  particles increasing the negative trend of the  $\zeta$  potential. Fig. 2 indicates a  $\zeta$  potential of about  $-60 \text{ mV}$  at high pH, however this potential is not enough to cause stabilization in the suspension as can be seen in Fig. 4(c).

On adding  $\text{NH}_4\text{PA}$  as dispersant, the  $\zeta$  potential decreases when concentrations less than or equal to  $2 \times 10^{-3} \text{ g}$  of dispersant/g of powder are used (Fig. 3), the decrement is more pronounced when the pH is acidic. It has been observed [24] that at low pH, the  $\text{NH}_4\text{PA}$  molecule is not ionized in an aqueous medium. The few ionized molecules have a negative charge in some of their monomers and they could be fixed on the positive sites in the surface of the  $\text{BaTiO}_3$  particles. In this way, some positive points are neutralized and the  $\zeta$  potential becomes more negative. When the pH is increased, the  $\text{NH}_4\text{PA}$  molecules are more easily ionized, therefore they repel each other and the adsorbed molecules become more rigid [24]. At high pH, the surface of the particles is highly negative so that adsorption of dispersant on the particles surface is more difficult, therefore the high pH curves in Fig. 3 do not decrease as much as they do at low pH. It should be noted, however that stabilization takes place at high pH (Fig. 6). This suggests that in spite of the net negative electric charge of the particles and dispersant molecules, there is some adsorption of the dispersant molecules on the particle surface, which is sufficient to cause stabilization.

#### 4.1.2. Sedimentation

The sedimentation tests showed that the suspensions are stable at high pH and relatively high concentrations of dispersant. When the pH is increased, less dispersant is necessary to stabilize the suspension (Fig. 6). At high pH values (10 and 11.3) and using concentrations equal to or higher than  $1.5 \times 10^{-3} \text{ g}$  dispersant/g powder, the final sediments are dense (Fig. 5) which indicates that the suspended particles can accommodate themselves in a compact manner, i.e., at these conditions the particles are better dispersed than in another conditions. An interesting feature is that at pH6 a small final sediment height is obtained (Fig. 5) which would indicate dispersion, however the sedimentation curves showed that there is not stabilization at this pH.

#### 4.1.3. Rheology

Several programs for application of shear rate on suspensions can be used, however the advantages and disadvantages of using either program are not clear [25].

In Fig. 7 it is evident that the fluid has a pseudoplastic behavior and that the thixotropy is very small since the increasing and decreasing shear rate curves coincide fairly well. This kind of “shear thinning” behavior has been interpreted as a result of the gradual breaking of the structures formed while the fluid was in repose, in such a way that a high shear stress is necessary to break them [26].

In order to observe the effect of the suspension parameters on the viscosity, the viscosity at a shear rate of  $10 \text{ s}^{-1}$  was chosen because this is approximately equal to the value applied during manual slip casting. As shown in Fig. 8(a), when the pH increases the viscosity decreases because the powder is better dispersed. On the other hand, by means of increasing the dispersant concentration, the adsorption of the  $\text{NH}_4\text{PA}$  molecules on the particles surface is incremented improving the powder dispersion and the viscosity also decreases [Fig. 8(b)]. Finally, on increasing the solid content [Fig. 8(c)] the traffic of particles during the flux increases so the viscosity also increases.

#### 4.1.4. Infrared spectroscopy

In the region from  $1520$  to  $1800 \text{ cm}^{-1}$  of the spectrum, the  $\text{NH}_4\text{PA}$  used in this work shows two peaks, one at  $1716 \text{ cm}^{-1}$  which is produced by the stretching vibrational mode of the  $\text{C}=\text{O}$  bond. The radical  $\text{NH}_4^+$  is initially bonded to the  $\text{C}=\text{O}$  but when the  $\text{NH}_4\text{PA}$  is in aqueous solution,  $\text{NH}_3$  evaporates leaving an  $\text{H}^+$  bonded to  $\text{C}=\text{O}$  [24] in such a way that electrical neutrality is maintained, so the peak at  $1716 \text{ cm}^{-1}$  has been interpreted as non ionized polymer [24]. The other peak is a band centered at  $1558 \text{ cm}^{-1}$ . This peak is produced by the vibrational stretching mode of the  $\text{C}-\text{O}$  bond that comes from the  $\text{COO}^-$  ion hence, this peak is interpreted as ionized polymer [24]. In fact, the  $\text{NH}_4\text{PA}$  shows another peak at  $\sim 1420 \text{ cm}^{-1}$  [24] but in this case this peak is overlapped by one of the strongest peaks of  $\text{BaTiO}_3$  centered at  $\sim 1450 \text{ cm}^{-1}$ . It can be observed in Fig. 9(b)–(c) that the peak at  $1716 \text{ cm}^{-1}$  is very clear at low pH indicating a non ionized state whereas the peak at  $1558 \text{ cm}^{-1}$  is more visible at high pH which indicates an ionized state. During adsorption of  $\text{NH}_4\text{PA}$  molecules onto the surface of  $\text{BaTiO}_3$  particles, the  $\text{NH}_4\text{PA}$  molecules could form a bidentate chelating or bidentate bridging with the Ba atoms on the particle surface [27].

#### 4.1.5. Slip casting

According to the stabilization map (Fig. 6), there is probably an excess of dispersant when a concentration of  $10^{-2} \text{ g dispersant/g powder}$  is used. Then, the dispersant molecules could act as obstacles to achieve an efficient accommodation of the powder particles during

casting, resulting in a low green density. Relative green densities of 62% have been reported using polyacrylic acid as dispersant with 45 vol% of solids [5], whereas in the present work,  $\sim 60\%$  was the highest average green density obtained using also 45 vol% of solid content.

## 5. Conclusions

1. Utilizing  $\text{NH}_4\text{PA}$  as dispersant, aqueous suspensions of  $\text{BaTiO}_3$  are dispersed at pH greater than or equal to 8, and dispersant concentrations greater than or equal to  $1.5 \times 10^{-3} \text{ g of dispersant/g of powder}$ . Electrostatic repulsion is not enough to cause dispersion.
2. An isoelectric point at  $\text{pH} \sim 2.5$  was found.
3. The viscosity of the suspensions decreases when the solid fraction diminishes and when the concentration of dispersant (between 0 and  $0.1 \text{ g dispersant/g powder}$ ) or the pH are increased.
4. Aqueous  $\text{BaTiO}_3$  suspensions behave as pseudo-plastic fluids.
5. The presence of  $\text{BaCO}_3$  was observed in sedimented powders of  $\text{BaTiO}_3$  and it was concluded that it is present as a contaminant.
6. Ammonium polyacrylate adsorbs at the surface of  $\text{BaTiO}_3$  particles at high pH. It was verified that the polyelectrolyte is ionized at these pH levels.
7. The use of  $10^{-2} \text{ g dispersant/g powder}$  caused a reduction of the relative green density as compared to the pieces prepared with  $2.5 \times 10^{-3} \text{ g of dispersant/g of powder}$ .
8. The highest green density (60%) was obtained at 45 vol% of solid content,  $\text{pH} = 11.5$  and  $2.5 \times 10^{-3} \text{ g dispersant/g powder}$ .

## References

- [1] J.M. Herbert, *Ceramic Dielectric and Capacitors*, Gordon and Breach Science Publishers, London, UK, 1985.
- [2] T.T. Fang, H.L. Hsieh, F.S. Shiau, *J. Am. Ceram. Soc.* 76 (5) (1993) 1205–1211.
- [3] M. Kuwaraba, H. Yanagida, in: S. Saito (Ed.), *Fine Ceramics*, Elsevier, USA, 1985, pp. 286–292.
- [4] J.S. Reed, *Introduction to the Principles of Ceramic Processing*, John Wiley & Sons, New York, 1988.
- [5] Z.C. Chen, T.A. Ring, J. Lemaitre, *J. Am. Ceram. Soc.* 75 (12) (1992) 3201–3208.
- [6] M.C. Blanco-López, B. Rand, F.L. Riley, *Key Engineering Materials* 132–136 (1997) 305–308.
- [7] M.C. Blanco-López, B. Rand, F.L. Riley, *Key Engineering Materials* 132–136 (1997) 301–304.
- [8] M.C. Blanco-López, B. Rand, F.L. Riley, *Key Engineering Materials* 132–136 (1997) 252–255.
- [9] J.H. Jean, H.R. Wang, *J. Am. Ceram. Soc.* 81 (6) (1998) 1589–1599.
- [10] M.V. Parish, R.R. Garcia, H.K. Bowen, *J. Mat. Sci.* 20 (1985) 996–1008.

- [11] K. Mikeska, W.R. Cannon, in: J.A. Mangels, G.L. Messing (Eds.), *Advances in Ceramics*, Vol. 9, Forming of Ceramics, The American Ceramic Society, OH, 1984, pp. 165–183.
- [12] R.J. Makinon, J.B. Blum, in: J.A. Mangels, G.L. Messing (Eds.), *Advances in Ceramics*, Vol. 9, Forming of Ceramics, The American Ceramic Society, OH, 1984, pp. 150–157.
- [13] R.J. Makinon, J.B. Blum, in: J.A. Mangels, G.L. Messing (Eds.), *Advances in Ceramics*, Vol. 9, Forming of Ceramics, The American Ceramic Society, OH, 1984, pp. 158–162.
- [14] Y. Hirata, M. Kawabara, *Mat. Lett.* 16 (1993) 175–180.
- [15] M. Hashiba, H. Okamoto, Y. Nurishi, K. Hiramatsu, *J. Mat. Sci.* 24 (1989) 873–876.
- [16] N. Shashidhar, J.R. Varner, R.A. Condrate Sr., in: G.L. Messing, S. Hirano, H. Hausner (Eds.), *Ceramic Transactions*, Vol. 12, Ceramic Powder Science III. The American Ceramic Society, OH, 1990, pp. 443–450.
- [17] Y. Hirata, A. Nishimoto, Y. Ishihara, *J. Ceram. Soc. Japan* 100 (8) (1992) 983–990.
- [18] A.R. Nyquist, O.R. Kagel, *Infrared Spectroscopy of Inorganic Compounds*, Academic Press, New York, 1971.
- [19] D.W. Fuerstenau, Pradip, R. Herrera-Urbina, *Colloids and Surfaces*, 68(1992)95–102.
- [20] D.A. Anderson, J.H. Adair, D. Miller, J.V. Biggers, T.R. Shrout, in: G.L. Messing, E.R. Fuller Jr., H. Hausner (Eds.), *Ceramic Transactions*, Vol. 1, Ceramic Powder Science II A. The American Ceramic Society, OH, 1988, pp. 485–492.
- [21] J.C.P. Schwartz, *Physical Methods in Organic Chemistry*, Oliver & Boyd, Edinburgh, 1968.
- [22] T. Hayashi, K. Satoh, K. Suganuma, personal communication.
- [23] K. Osseo-Asare, D.W. Fuerstenau, *Int. J. Min. Proc.* 7 (1980) 117–127.
- [24] D.H. Lee, R.A. Condrate Sr., J.S. Reed, in: J.H. Adair, J.A. Cassey, C.A. Ransall, S. Venigalla (Eds.), *Ceramic Transactions* Vol. 54, Science, Technology and Applications of Colloidal Suspensions. The American Ceramic Society, 1995, pp. 67–81.
- [25] C. Galasi, E. Rastelli, R. Lapasin, in: J.H. Adair, J.A. Cassey, C.A. Ransall, S. Venigalla (Eds.), *Ceramic Transactions* Vol. 54, Science, Technology and Applications of Colloidal Suspensions. The American Ceramic Society, 1995, pp. 3–21.
- [26] L. Bergström, in: R.J. Pugh, L. Bergström (Eds.), *Surface and Colloidal Chemistry in Advanced Ceramic Processing*, Marcel Dekker, New York, 1994, pp. 193–244.
- [27] J.M. Saniger, H. Hu, V.M. Castaño, J. García-Alejandre, in: J.H. Adair, J.A. Cassey, S. Vaeigalla (Eds.), *Handbook on Characterization Techniques for Solid–Solution Interface*, The American Ceramic Society, OH, 1993, pp. 169–176.